

SANDWICH: Towards an Offline, Differentiable, Fully-Trainable Wireless Neural Ray-Tracing Surrogate

Yifei Jin

KTH Royal Institute of Tech. & Ericsson AB
Stockholm, Sweden
yifeij@kth.se

Ali Maatouk

Yale University
New Haven, USA
ali.maatouk@yale.edu

Sarunas Girdzijauskas

KTH Royal Institute of Tech.
Stockholm, Sweden
sarunasg@kth.se

Shugong Xu¹

Xi'an Jiaotong-Liverpool University & Shanghai University
Suzhou & Shanghai, China
shugong@xjtlu.edu.cn

Leandros Tassioulas

Yale University
New Haven, USA
leandros.tassioulas@yale.edu

Rex Ying

Yale University
New Haven, USA
rex.ying@yale.edu

Abstract—Wireless ray-tracing (RT) is emerging as a key tool for three-dimensional (3D) wireless channel modeling, driven by advances in graphical rendering. Current approaches struggle to accurately model beyond 5G (B5G) network signaling, which often operates at higher frequencies and is more susceptible to environmental conditions and changes. Existing online learning solutions require real-time interaction with radio environment during training, which is both costly and incompatible with GPU-based processing. In response, we propose a novel approach that redefines ray trajectory generation as a sequential decision-making problem, solved with the proposed Scene-Aware Neural Decision Wireless Channel Raytracing Hierarchy (SANDWICH) approach. The SANDWICH approach leverages a decision transformer to jointly learn the optical, physical, and signal properties within each designated environment in a fully differentiable approach, which can be trained entirely on GPUs. SANDWICH offers superior performance compared to existing online learning methods, and outperforms the baseline by $4e^{-2}$ rad in RT accuracy. Furthermore, channel gain estimation w.r.t predicted trajectory only fades 0.5 dB away from using ground truth wireless RT result for channel gain estimation.²

Index Terms—Wireless Raytracing, RF Sensing, Channel Modeling, Channel Generation

I. INTRODUCTION

In the B5G/6G era, high-fidelity wireless channel modeling has become indispensable for advancing wireless systems. Recent studies in Joint Communication And Sensing (JCAS) [1], beam management [2], and positioning [3] have underscored the necessity of accurately modeling wireless signal interactions within radio environments. Supported by computational Electro-Magnetic (EM) theory and Geometrical Optics (GO). Recent research [4–11] introduces wireless RayTracing (RT) to capture these interactions through a Shoot-and-Bounce Sequence (SBS) [12]. SBS is widely used in ray-tracing where rays are “shot” from a source and traced as they interact with surfaces through reflection, diffraction, and penetration.

¹The author was with the Shanghai University, Shanghai, China. He is now with the Xi'an Jiaotong-Liverpool University, Suzhou, China.

²This work was partially supported by the Wallenberg AI, Autonomous Systems and Software Program (WASP) funded by the Knut and Alice Wallenberg Foundation. The implementation is available at www.github.com/bluelancer/SANDWICH

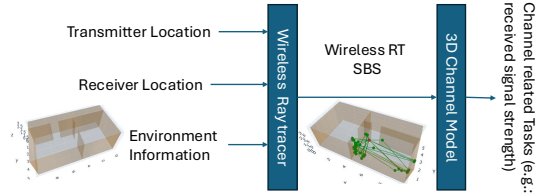


Figure 1. Workflow of Genuine Wireless Raytracer: Wireless Raytracer takes the input of Tx, Rx location, and radio environment information, and outputs SBS to be further utilized on wireless channel-related tasks.

Wireless RT effectively models the EM wave propagation and scattering in a complex environment³, while adhering to GO and the Uniform Theory of Diffraction (UTD) [4]. Despite its potential, wireless RT involves computationally expensive raytracer [13], which calculates a set of SBS relevant for wireless reception, from infinite GO & UTD-feasible rays. In the data-driven channel modeling approach, such SBS set is a robust prior for a range of channel-related applications, as illustrated in Fig. 1. We interchangeably refer to “wireless RT ray trajectory” and SBS throughout this work.

A. Wireless RT Surrogate

Recently, research has been exploring neural methods as wireless RT surrogates [4, 7, 14] to estimate SBS, aiming to reduce the computational costs of traditional wireless ray tracers with scalability towards new Tx, Rx location. However, wireless RT is typically formulated as a sparsely-supervised and non-differentiable learning objective with Out-Of-Distribution (OOD) samples, for the following three reasons: 1) The indeterminate length of SBS and its interactions with the environment before its receipt by Rx; 2) Due to the nature of the wireless signal, wireless RT SBS is not differentiable on the 2D plane of the environment. 3) Similar to a genuine raytracer, the surrogate should be capable of handling unseen transmitter (Tx) & receiver (Rx) locations in the 3D space.

³In this paper we mainly refer to indoor scenario.

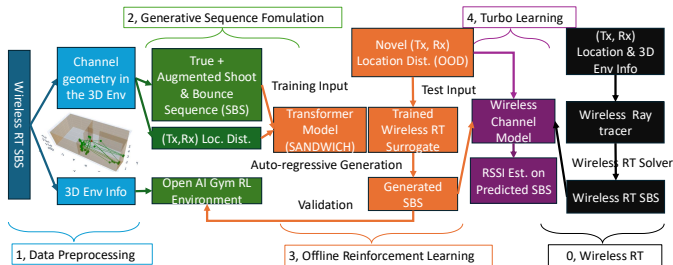


Figure 2. Schematic Representation of SANDWICH: 1, Segment wireless RT and 3D environment. 2, Sequentialize RT result into SBS. 3, Train neural surrogate & apply auto-regressive generation. 4, Apply generated RT to the wireless channel model. Such workflow serves as a neural surrogate of 0, a wireless RT process.

Several approaches have been proposed in the literature to address such challenges. For example, Orekondy, Kumar, et al. [7] introduced WINERT, which mimics the output of a wireless ray tracer at each interaction with a greedy policy, using temporal difference (TD) learning.

While being capable of partially replacing a genuine raytracer with time & computational superiority, existing methods are hindered by several significant limitations: 1) **Online Supervision**: Dependence on real-time feedback from radio environment modeling and ray-tracer in training loop; 2) **Vectorization**: Inability to process batches of rays efficiently, coupled with GPU incompatibility; 3) **Differentiability**: The existing method adapts the ray tracer to feed the state space to determine the next action, segmenting the radio environment into several discontinuous state spaces and neglecting their sequential relation, which leads to exploding gradients during training.

B. Proposed Method

This paper addresses wireless RT considering Tx/Rx locations and signal-surface interaction in indoor environments with surface texture information. To capture “state space continuity”, we reformulate the wireless RT as a sequence generation problem [15]. Inspired by the recent success of offline Reinforcement Learning (RL) algorithms like Decision Transformer(DT) [16], we propose a novel Scene-Aware Neural Decision WIREless Channel raytracing Hierarchy (SANDWICH) model. The method models “state space continuity” and allows learning from a limited set of collected RT results without assumptions on the radio environment or supervision density. Specifically, SBS representing a wireless ray can be generated similarly to token sequences, utilizing the transformer’s [17] capability of learning relational attention within the token sequence. We house the sequence auto-regressive generation task within an offline RL scheme, enforcing the model to internalize the radio environment as a constraint during SBS generation, to unhook the requirement for online supervision from well-parameterized radio environment in State-Of-The-Arts (SOTA).

We illustrate a schematic representation of the proposed solution in Fig. 2, including four major steps: 1) Segment raw data into 3D environment and channel information. The ray’s trajectory is also transformed into true & augmented

SBS for transformer models. 2) Create tailored OPENAI GYM environment for test-time verification with OOD Tx & Rx locations. 3) Train the proposed model and generate SBS on novel (Tx, Rx) distribution. 4) Besides the generated wireless RT geometrical accuracy, the generated SBS are utilized as priors for channel model, to enhance performance in downstream tasks within a Turbo Learning [18] framework.

Our method leverages a customized DT [16] to integrate sparse supervision through expected returns through a novel sequential decision-making formulation for Markov Decision Process (MDP), thereby decoupling the need for continuous online supervision from the environment. Additionally, we propose a data augmentation technique based on Fibonacci sphere [19] to generate stochastic trajectories that enhance generalization of DT on OOD test samples, alongside state supervision to enforce environment awareness.

C. Our Contribution

1) We propose an end-to-end GPU-trainable, fully differentiable, and vectorizable SANDWICH framework for wireless RT. 2) In addition, we propose to augment the training rays by sampling from Fibonacci Spheres, that proven to strengthen the generalization performance. 3) we also propose to distill the optical properties of materials to the model by predicting the interaction type. 4) Our approach outperforms the online learning solution by $4e^{-2}$ rad in RT accuracy and only fades 0.5 dB away from GT-ray-powered channel gain estimation, while outperforming all non-RT based baselines with generated wireless RT results.

II. RELATED WORK

A. Wireless 3D Channel Modeling

Wireless RT is a specialized subfield within wireless channel estimation, particularly relevant in 3D environments where millimeter-wave (mm-wave) propagation can be statistically described as [20]

$$h(t, \Theta, \Phi) = \sum_{r_k \in \{r_k\}} a_k(t) \delta(t - \tau_k(t)) \delta(\Theta - \Theta_k(t)) \delta(\Phi - \Phi_k(t)) \quad (1)$$

In (1), a wireless channel is represented by a set of rays (denoted as $\{r_k\} := \{r_1, \dots, r_k\}$, with cardinality $|\{r_k\}| = K$). Each ray r_k is characterized by its signal gain $a_k(t)$, one-way delay $\tau_k(t)$, and phase $\Theta_k(t), \Phi_k(t)$ for arrival and departure angle, respectively, expressed using Dirac function δ . These parameters summarize the property of SBS, which includes a series of ray-surface interactions, in the radio environment F .

B. Heuristic Wireless RT

Recent research has focused on wireless RT estimation in a 3D environment and application to physics-informed channel modeling [3]. Geok, Hossain, et al. [10] offers a comprehensive review of the heuristics method and discusses such methods’ complexity and generalization limitations. [5, 21] offers heuristics-method-driven simulator in 3D environment, which has been proved by Orekondy, Kumar, et al. [7] to be time and computational expensive. Hoydis, Aoudia, et al. [4] and Choi, Oh, et al. [6] proposed a SBS-based simulator that greatly

accelerates the simulation speed through highly efficient Monte-Carlo rays integration while dependent on online supervision from the environment through a designated ray-tracing engine. SANDWICH builds upon insights from heuristic from Hoydis, Aoudia, et al. [4] and Geok, Hossain, et al. [10], with the concepts of SBS and early-step-focused-rewarding to mitigate bias propagation within a generative portfolio [22].

C. Neural Wireless RT

In the past year, researchers have been distilling the complex heuristic (or parts of it) into neural surrogates for real-time Wireless RT results [11, 18, 23], where [18, 23] adapt Neural Radiance Field (NeRF) to extract 3D mesh from RGB images while [11] incorporate an online learning formulation. The closest work to ours is by Orekondy, Kumar, et al. [7], where the authors proposed WINERT based on a TD-learning approach to distilling wireless RT. However, their method is not vectorizable, not GPU trainable, and supervised by online feedback from the radio environment. Recent work [24, 25] has avoided wireless RT but attempted to model RF signal strength distribution from a probabilistic perspective without SBS prior, while this goes beyond the scope of wireless RT surrogate and does not capture the full wireless propagation physics. We consider SANDWICH shares the strength of [7, 11, 26] through a novel generative formulation of wireless RT problem while being offline, fully differentiable, and vectorized-trainable with scene-awareness. Instead of decoupling the SBS into densely populated rewards, our approach generates SBS in an auto-regressive generation manner, spanning the sparse-reward signal through the whole SBS trajectory.

D. MDP on Wireless RT

Given the locations of the Tx and Rx, denoted by $\text{loc}(Tx)$ and $\text{loc}(Rx)$ respectively, a set of rays $\{r_K\}$ are emitted from Tx and interacts with F through a designated simulator \mathcal{S} until received at Rx [5, 21]. Following the work in [7], the RT training formulation can be done through an MDP $(\mathbf{S}, \mathbf{A}, \mathbf{P})$, decomposing each ray in SBS set $r_k \in \{r_K\}$ into a sequence of state-action-interaction triplets $[(s_i, a_i, t_i)]$, state space $s_i \in \mathbf{S} \subset \mathbb{R}^3$, action space $a_i \in \mathbf{A} \subset SO(3)$, where $SO(3)$ denotes 3D rotation group, and transition dynamics \mathbf{P} . Each state s_i represents the coordinate of a ray in its trajectory, while each action $a_i = (\phi, \theta) \in \mathbf{A}$ denotes the radian ϕ and azimuth θ out-angle relative to the previous hop s_{i-1} . The interaction t_i at each state s_i can be categorized into three types: reflection (\mathcal{R}), diffraction (\mathcal{D}), and penetration (\mathcal{P}) that attributes on s_i as property of wireless signals. The transition function is defined as $\mathbf{P}(s_{i+1}|s_i, a_i) = \mathcal{S}(F, s_i, a_i)$ through \mathcal{S} as collected experience in SBS. A logic-based receiver classifier $\text{Rec}(Rx, F, \{r_K\})$ determines if the rays in $\{r_K\}$ successfully reach the Rx. The objective is to learn a greedy policy π_{out} that predicts identical ray set $\{r_K\}$ on new $\text{loc}(Tx)$, $\text{loc}(Rx)$ combined with \mathcal{S} as transition dynamics \mathbf{P} , such formulation is outlined in Fig. 3a.

III. PROBLEM FORMULATION

A. Challenge in MDP Formulation

MDP formulation of wireless RT integrates several inherent challenges: 1) **Sparse Supervision/reward**: Reward signals are

granted on receipt of each SBS, spanning across a sequence of decisions, leading to sparse supervision. 2) **Non-differential Objective**: Wireless ray propagation is influenced not only by the locations and configurations of the Tx and Rx but also by the 3D structure and texture of the environment. Consequently, wireless RT results may not be differentiable in a 2D plane, emphasizing the need for a sequential representation-based learning approach. 3) **OOD Samples in S**: To demonstrate the generalization capabilities of the proposed model, the test environment includes novel Tx and Rx locations $\text{loc}(Tx)$, $\text{loc}(Rx)$, resulting in an extrapolated state space. This highlights the necessity of incorporating F as an inductive bias.

B. Limitation on Alleviation Approaches

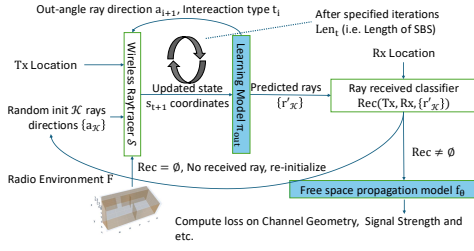
Although some SOTA methods [4, 7] can alleviate such challenges, however these alleviations themselves introduce new problems: 1) **Densifying the reward signal on a per-action basis**: MDP formulation densifies such rewards by learning a greedy policy π_{out} that predicts the next action a_{i+1} and current type t_i with barely current state s_i , and action a_i . This often introduces heuristic and non-differentiable components \mathcal{S} and Rec in training time as non-trainable components. Moreover, ray length Len_k has to be specified which leaks information during test time; 2) **Excessive exploring F** : SOTA methods emits a large number of rays $\{r_K\}$, where $|\{r_K\}| = \mathcal{K} \gg K$, to explore the reward distribution in F through online supervision from \mathcal{S} ' feedback. **We argue that the excessive computation is caused by the fact that the SBS ray generation process, is not physically a markov process.** Hence modeling it with an MDP necessitates excessive sampling and post-trajectory pruning with Rec . These approaches incur significant computational overhead, create incompatibility on GPU due to \mathcal{S} involvement, and rely on online supervision.

In contrast, this paper formulates the wireless RT task as **an end-to-end learning model to retrieve the set of SBS for OOD Tx & Rx location, acquired by a wireless raytracer**, which leads to an offline, fully GPU-trainable method (SANDWICH) that learns wireless RT through a generative scheme.

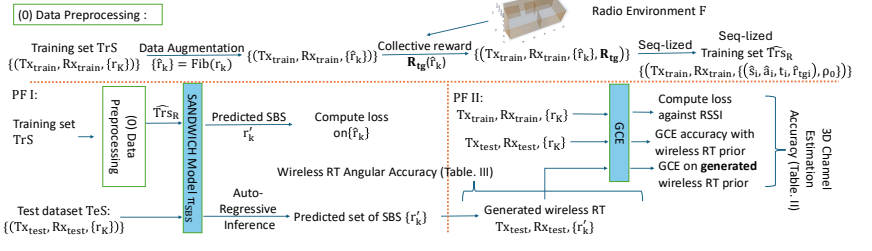
C. Proposed Problem Formulation

In this work, we introduce two novel problem formulations (PF) following previous acronyms: **PF I**: Given MDP $(\mathbf{S}, \mathbf{A}, \mathbf{P}, \mathbf{R}_{tg}, \rho_0)$, we consider each SBS r_k to be summarized as $[(s_i, a_i, t_i)]$, with length Len_k and deterministic transition \mathbf{P} from collected wireless RT results. \mathbf{R}_{tg} is a set-based reward function evaluates a predicted SBS r'_k against GT set $\{r_k\}$, and ρ_0 denotes the initial action distribution. The objective is to find a policy π_{SBS} that generates SBS r'_k , maximizing the expected return $E(\mathbf{R}_{tg}(r'_k))$.

Additionally, to validate the utility of fully-generated wireless RT sequences $\{r'_k\}$, we incorporate a secondary problem formulation through *Turbo Learning*: **PF II**: We train a ‘‘Golden Channel Estimator’’ (GCE) h'_G using data-driven approach [27] to simulate $h(t, \Theta, \Phi)$ in (1). This is done by summarizing $\{r_k\}$, F , Rx , Tx , and their respective locations $\text{loc}(Tx)$ and $\text{loc}(Rx)$ all as inputs to the estimator. We conduct a hyperparameter search to optimize the GCE for its best possible



(a) Schematic Representation of Problem Formulation in [7]: (a.1) Given Tx location and \mathcal{K} randomly initialize ray direction $\{a_{\mathcal{K}}\}$, \mathcal{S} outputs the state s regarding the intersection of $\{a_{\mathcal{K}}\}$ and F . (a.2) The greedy policy π_{out} was trained by iteratively collecting next-state s_{t+1} from \mathcal{S} to suggest current type and next direction. (a.3) Once the designated length Len_k is reached, a logic-based ray receipt classifier Rec will filter the predicted SBS proximate to Rx location. The training is constrained to be batch size 1 to ensure greediness.



(b) Schematic Representation of Proposed Problem Formulation: (b.1) A collected set of SBS is augmented, attributed with collective reward, and sequentialized to be adapted to sequential-decision-making formulation. (b.2) In **PF I**, the learning policy π_{SBS} takes observation on the whole SBS, with a seq2seq training scheme. (b.3) In test time, π_{SBS} takes the input of OOD Tx & Rx and is promoted to generate the sequence with maximum collective reward. The generated $\{r'_k\}$ will be used in **PF II**. (b.4) To compare the usability of generated SBS, we compare the generated $\{r'_k\}$ and GT $\{r_k\}$ through a well-trained GCE and offer precision and error distribution analysis.

Figure 3. Comparison of Problem Formulations on Learning Wireless RT Surrogate: Each blue box denotes a trainable component and the white box denotes a non-trainable component.

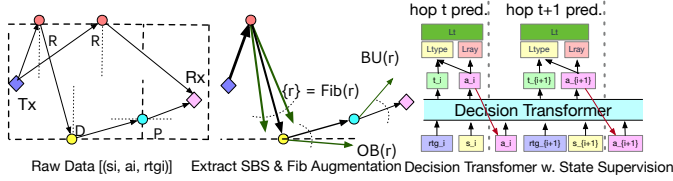


Figure 4. Component in SANDWICH Training Pipeline (i.e. **PF I** in Fig. 3b): *i*) SBS Sequentialization: Given a set of SBS from Tx to Rx in wireless RT result, each SBS is parsed into a decision sequence, with interaction type (noted as differently colored shapes) attributed on each step. *ii*) Per-SBS Fib Augmentation: For each SBS, we applied $\mathbf{Fib}(r_k)$ to augment a diverse quality of SBS, and compute collective reward \mathbf{R}_{tg} as their quality metric. *iii*) Train SANDWICH through the augmented & shuffled SBS: apply seq2seq training on the input sequence $\{s_i, a_i, r_{tgi}\}$, against output sequence $\{t_i, a_{t+1}\}$ regards to loss function L_t .

channel estimation. We then compare the performance and error (KL-divergence) with predicted $\{r'_k\}$ against the GT $\{r_k\}$ on channel estimation task using GCE. Both PFs are tested against novel distribution of (Tx, Rx) on extrapolated feature space to prove its generalization performance. We summarize the differences between our problem formulation and previous works in Fig. 3, and summarize the defined notation in Table. I.

IV. METHODOLOGY

The key idea is to **keep track of the historical states in each SBS to improve sampling efficiency when collecting experience from radio environment**. This is critical to handle the sparse rewards of wireless RT within an offline RL framework, as the expected return is granted for the whole SBS, outlined in **PF I**.

Modeling SBS as a sequence aligns with optical ray tracing techniques like *path tracing* [28], which Keller, Viitanen, et al. [29] demonstrated to be more precise than per-hop ray-surface interaction modeling, albeit computationally impractical for

real-time rendering. Wireless RT strikes a balance, as noted by Kajiya [30]: while path-tracing a finite number of rays is computationally expensive, it remains feasible and sufficient for downstream tasks (e.g., multi-path modeling), enhancing ray rendering precision. Such insight diverges from greedy policy's state embedding [7], (Tx,Rx)-conditioned embedding [27, 31], or upsampling methods used to densify existing RT results [32] in previous works.

A. Decision Transformer

DT [16] is promising for handling sequential decision-making by referencing all prior decisions within a sequence. As formulated in **PF I**, each SBS is represented as a token sequence, where each step is defined by a triplet of its state, action, and return $(s_i, a_i, r_{tgi}) \in (\mathbf{S}, \mathbf{A}, \mathbf{R}_{tg})$. For a fair comparison, we input the sequence of all preceding steps $[(s_i, a_i, r_{tgi})]_i$ up to hop i , masking the current action a_i to predict the current hop's action and interaction type t_i , as [7] did. At test time, DT models leverage the expected return $E(\mathbf{R}_{tg}(r'_k))$ to perform auto-regressive generation for OOD test inputs, defined by $\text{loc}(Tx)$ and $\text{loc}(Rx)$, against generated ray r'_k . The return function \mathbf{R}_{tg} represents a cumulative reward for future steps, extending beyond the greedy reward used in MDP formulation (i.e.: illustrated in 3a). \mathbf{R}_{tg} also incorporates a near-differentiable RT precision metric to guarantee optimal generation precision. This approach frames wireless RT as a differentiable, end-to-end sequential decision-making problem, as illustrated in Fig. 4.

B. Fib Augmentation

DT shares a suboptimal generalization performance as per [33, 34], especially in SBS testset including OOD Tx, Rx locations. Moreover, wireless RT SBS only includes positive samples, without null samples to shape the action space. Inspired by Rogne [19], we introduce a data augmentation scheme, $\mathbf{Fib}(r_k)$, leveraging the Fibonacci sphere to improve

Table I
TABLE OF NOTATIONS

Wireless 3D Channel Modeling Notation:	
$h(t, \Theta, \Phi)$	Wireless channel response
r_k	A single ray in the wireless RT result $\{r_k\}$
K	Cardinality of the set of rays $\{r_k\}$ for $h(t, \Theta, \Phi)$
$a_k(t), \tau_k(t)$	Signal gain, time delay of the ray r_k at time t
$\Theta_k(t), \Phi_k(t)$	Angular parameters of the ray r_k at time t
$\delta(\cdot)$	Dirac delta function
$loc(Tx), loc(Rx)$	Locations of the transmitter and receiver
F	Wireless radio environment
MDP with TD-Learning Formulation Notation:	
$\{r_{\mathcal{K}}\}$	A large number of ray attempts (i.e. $ \{r_{\mathcal{K}}\} = \mathcal{K} \gg K$) for TD Learning
$(\mathbf{S}, \mathbf{A}, \mathbf{P})$	State space, Action space and Transition dynamics
(s_i, a_i, t_i)	State, action, interaction triplets of the ray at step i
$P(s_{i+1} s_i, a_i)$	Transition function of moving to state s_{i+1} , realized by designated ray-tracer/RT Simulator $\mathcal{S}(F, s_i, a_i)$
$\pi_{out}(s_i, a_i)$	TD-Learning policy for predicting next ray direction a_{i+1} and current interaction type t_i
$R(s_i, a_i)$	Reward function at state s_i for action a_i
ρ_0	Initial action distribution
Len_k	Length of the ray's shoot-and-bounce sequence (SBS)
r_k	Full SBS trajectory of the ray k : $[(s_i, a_i, t_i)]$
$Rec(Rx, F, \{r_k\})$	Receiver classifier for determining valid rays
Sequential Decision-Making Formulation Additional Notation:	
$\pi_{SBS}(Tx, Rx, \rho_0)$	Neural sequential policy for generating SBS
$\{r'_k\}$	Generated ray set by SANDWICH
$\hat{r}_k = \mathbf{Fib}(r_k)$	Augmented SBS \hat{r}_k using Fibonacci sphere, from each sample r_k in training set.
$\sigma_\phi, \sigma_\theta$	Variance in Fibonacci augmentation
$\mathbf{R}_{tg}(r'_k)$	Collective reward for the generated ray r'_k , $r_{tgi} \in \mathbf{R}_{tg}(r'_k)$ for each step $i \in [L_k]$, also applied on \hat{r}_k .
$R_{SBS}(r'_k, \{r_k\})$	Set-based fitness for r'_k against $\{r_k\}$ to parameterize $\mathbf{R}_{tg}(r'_k)$, consists of L_{ray} and P_\perp , also applied on \hat{r}_k against $\{r_k\}$ for augmented sample's fitness.
$L_t(r'_k, F)$	Training loss of SANDWICH, parameterized by L_{ray} , $L_{[type]}$ and weighting α
$L_{ray}(r_k, r'_k)$	Set-based loss on SBS geometrical fitness
$L_{[type]}(t_i, t'_i)$	Cross-entropy loss on t_i
$P_\perp(r'_k, F)$	Geometric correctness penalty, consists of BU, OB, TE
$BU(\{(a_j, t_j)\})$	Geometric consistency penalty at step j
$OB(r'_k, F)$	Outbound penalty function for r'_k regarding F
$TE(r'_k, Rx)$	Terminal error for r'_k

sampling efficiency from radio environment with non-trivial exploration dynamics. We generate a batch of normal Fibonacci spheres for each a_j and sampled a set of augmented ray $\mathbf{Fib}(r_k) = \{[(\hat{a}_j, t_j)]_k\}$ by introducing tunable variances $(\sigma_\phi, \sigma_\theta)$ around (ϕ, θ) . The set of augmented ray is shuffled together with SBS GT to form a training set of SBS:

$$\{\hat{r}_k\} := \{r_k\} \cup \left\{ \bigcup_{r_k \in \{r_k\}} \mathbf{Fib}(r_k) \right\} \quad (2)$$

C. Reward Shaping

To offer a near-differentiable reward measure \mathbf{R}_{tg} [16], we propose a novel fitness function $R_{SBS}(\hat{r}_k, \{r_k\})$ to formulate the collective reward $\mathbf{R}_{tg}(\hat{r}_k)$. We expect R_{SBS} to measure $\{\hat{r}_k\}$ from both RT precision and geometry constraints in radio environment:

$$\begin{aligned} \mathbf{R}_{tg}(\hat{r}_k) &:= R_{SBS}(\hat{r}_k, \{r_k\}) \\ &= -\operatorname{argmin}_{r_k \in \{r_k\}} [L_{ray}(r_k, \hat{r}_k) - P_\perp(\hat{r}_k, F)] \end{aligned} \quad (3)$$

In (3), L_{ray} is an angular set-based loss that supervises the RT precision scale:

$$L_{ray}(r_k, \hat{r}_k) = \sum_{j \in [L_k]} w_j \log(|a_j - \hat{a}_j|), \quad a_j \in r_k. \quad (4)$$

In (4), w_j is a heuristic reverse sequential weight to encourage the transformer to learn the Markovian properties of the sequence. Unlike an increasing weighted reward in Vanilla DT, this decreasing weighted reward emphasizes supervision on the closest match to the GT SBS during the early generation steps. This approach helps avoid a trivial solution that could arise between two optimal SBS. On the other hand, P_\perp supervises the geometry constraints:

$$P_\perp(\hat{r}_k, F) = \text{OB}(\hat{r}_k, F) + \sum_{j \in |\hat{r}_k|} \text{BU}(\hat{a}_j, t_j) + \text{TE}(\hat{r}_k, Rx). \quad (5)$$

In (5), $\text{OB}(\hat{r}_k, F)$ penalizes any outbound attempts by \hat{r}_k from F . The term $\text{TE}(\hat{r}_k, Rx)$ introduces a penalty e^d , where $d \geq d_0$, if \hat{r}_k misses $\text{loc}(Rx)$ by a tunable distance d_0 . Lastly, $\text{BU}(\hat{a}_j, t_j)$ ensures geometric consistency between (\hat{a}_j, t_j)

$$\text{BU}(\hat{a}_j, t_j) = \begin{cases} \operatorname{argmin}_{ax} [|\mathbb{1}_{ax} \hat{a}_j| - |\mathbb{1}_{ax} \hat{a}_{j-1}|] & \text{if } t_j = \mathcal{R} \\ -10 & \text{if } t_j = \mathcal{P}, \hat{a}_j \neq \hat{a}_{j+1} \\ 0 & \text{otherwise.} \end{cases} \quad (6)$$

In (6), \hat{a}_j is the directional vector defined by \hat{a}_j , while $\mathbb{1}_{ax}$ denotes a set of unit vectors along the 3D axes.

R_{SBS} aligns the expected return \mathbf{R}_{tg} from DT with wireless RT precision while addressing geometry constraints. Such correspondence fitness is inspired by the adversarial clustering method described in [35]. The holistic metric of SBS augmentation samples enables DT to learn a sequential action space for SBS, decouple the requirement of collecting per-action reward from simulators (in contrast to [7, 36]), and empowers vectorization and GPU-training.

D. Optimization

Finally, we formulate the training loss $L_t(r'_k, F)$ of SANDWICH against each predicted SBS r'_k :

$$L_t(r'_k, F) = \operatorname{argmin}_{r_k \in \{r_k\}} \left[\alpha L_{ray}(r_k, r'_k) + \sum_{i \in [L_k]} L_{[type]}(t_i, t'_i) \right] \quad (7)$$

$L_{[type]}(t_i, t'_i) = \text{CROSSENTROPY}(t'_i, t_i)$ where α is a hyperparameter. Additionally, we incorporate state supervision $L_{[type]}$ into the backbone DT to enforce surface texture during ray interactions, inspired by DADT. [33].

We show the effectiveness of novel components, $\mathbf{Fib}(r_k)$ and $L_{[type]}$, contribute SANDWICH performance in Sec. V. The aforementioned building blocks are housed in an end-to-end training pipeline, referenced in Fig. 4: *i*) SBS Sequentialization: We segment each r_k into a sequence of action and state type $[(a_j, t_j)]_k$. *ii*) Fib Augmentation: We generate a batch of normal Fibonacci spheres for each a_j and sampled a set of augmented ray $\mathbf{Fib}(r_k) = \{\hat{r}_k\}$. *iii*) Decision Sequence Formulation: We apply R_{SBS} to \mathbf{R}_{tg} for the augmented dataset, shuffled with GT. We pad the wireless RT SBS with zero sequence to a uniform length and apply DT. *iv*) State supervision ($L_{[type]}$): In addition to training against $L_{ray}(r_k, r'_k)$, we introduce additional set-based supervision on a type readout of each step t'_i in r'_k , against GT interaction type t_i attributed on respective state s_i .

Table II
COMPARISON OF MAE AND KL DIVERGENCE BETWEEN MODELS AND GT/GCE ACROSS THE TESTSETS

Metric (dB)	MAE(Model, GT)			MAE(GCE, Model)			KL_div(pdf(GCE)-pdf(Model))		
On Test set:	Checkerboard	Genz	GenDiag	Checkerboard	Genz	GenDiag	Checkerboard	Genz	GenDiag
GCE (Topline)	3.422	3.181	3.039	0	0	0	0	0	0
SANDWICH (Proposed)	3.966	3.804	3.689	1.494	1.640	1.422	0.0410	0.0534	0.0317
MLP(Reproduced)	5.337	5.846	4.729	3.760	4.291	3.496	0.2827	0.6003	0.1913
KNN(Reproduced) 1	11.21	11.04	4.412	9.856	9.939	4.963	0.1447	0.1565	0.1468
KNN(Reproduced) 2	10.71	10.59	4.180	9.446	9.542	4.822	0.1431	0.1516	0.1508

V. EXPERIMENTS

We train SANDWICH and other baseline models for environments from the SOTA DeepLayout [37]. We create a standalone GYM environment for each layout and test against 3 test sets [CHECKERBOARD, GENZ, GENDIAG], as introduced in [7]. CHECKERBOARD only includes OOD Tx sample, with identical Rx location, GENZ introduces Rx locates on a different horizontal plane, while GENDIAG introduces Rx location from a novel distribution in the 3D environment. All test sets include 15 novel Tx locations and approximately 1800 Rx locations, each (Tx, Rx) pair includes at most 30 possible rays. ⁴

A. Ablation Against Decision Transformer Families

To prove the effectiveness of introduced novel building blocks, we conduct an ablation study against vanilla DT (train against L_{ray}) and DT with L_t . We train with the same hyper-parameter, test against all three test sets, and compare the best baseline from [7] as a reference in Fig. 5. Both the $\mathbf{Fib}(r_k)$ and $L_{[type]}$ contributes to SANDWICH's superior performance over vanilla DT and baselines. Also, due to bias propagation in generation task [22], applying $L_{[type]}$ and $\mathbf{Fib}(r_k)$ can restrain such degradation when path length increases.

B. Wireless RT: Geometrical Accuracy

We consider the performance of wireless RT accuracy by mean averaged angular loss in all three test sets. We compare our proposed solution against claimed and reproduced baselines in [7]. As no code was available for reproducing the baselines, for MLP baseline [27, 31], we consider a hyper-parameter search scheme towards downstream tasks for non-provided hyperparameters, i.e.: batch size, number of epochs, and formulation of angular supervision. For KNN baselines [32], we offer 2 forms of reproduction 1) We reproduce according to [7] which offers an $n=1$ matching within Tx and Rx between train and test sets. 2) We run $n=6$ KNN and pick the best-performing neighbor for angular loss, this upper-bounds the vanilla KNN reproduction performance as per claimed in [32]. For WINERT baseline, the logic component is not provided so we only apply claimed performance. We show that the proposed SANDWICH outperforms the previous baseline method in different generalizations of (Tx, Rx) locations. Although reported as SOTA, [24] is not included

⁴Orekondy, Kumar, et al. [7] introduced 3 new environments in "WIIDOR" besides the 100 used environments in "WI3ROOM". However, since its building block [21] is proprietary software, we only use "WI3ROOM" from DeepLayout [37] as baseline dataset.

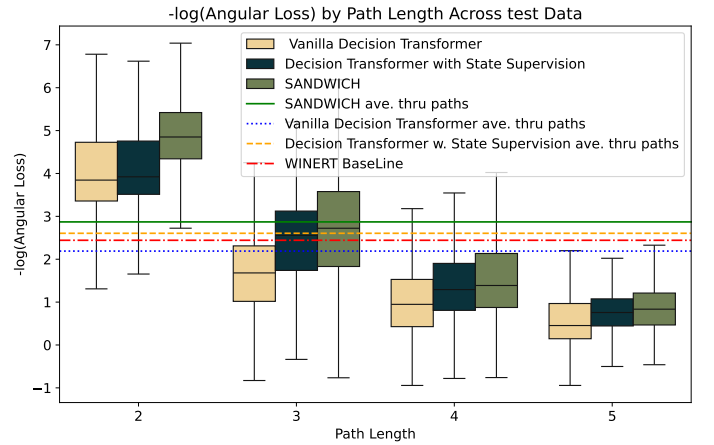


Figure 5. Ablation of SANDWICH against Vanilia DT [16] and DT with state supervision L_t [33].

in the comparison as they have not been open-sourced for either dataset or source code, making it impossible to ensure fairness.

Table III
COMPARISON OF WIRELESS RT ANGULAR ACCURACY

Angular Loss (MAE, rad)	Checkerboard	Genz	GenDiag
SANDWICH (Proposed) ²	0.0464	0.052	0.0372
WINERT (Claimed in [7])	0.087	0.084	0.085
MLP(Claimed in [7])	0.33	0.35	0.322
KNN(Claimed in [7])	0.212	0.226	0.213
MLP(Reproduced)	0.504	0.518	0.497
KNN(Reproduced 1)	0.509	0.545	0.275
KNN(Reproduced 2)	0.470	0.512	0.247

C. Turbo learning: RT as a prior for RSSI estimation

Finally, we consider using generated rays as prior for received signal strength indicator (RSSI) prediction to examine the usability of wireless RT. The GCE serves as a topline that takes GT wireless RT as input, which bounds the best capability of the GCE. We apply the generated ray through SANDWICH to GCE and compare it against the topline and non-wireless RT-based solutions, with their implementations the same as in Table III. In Table II, we show that SANDWICH generated

²For $L_k = 1$ ray is considered well received, as no learning model is applied.

ray provides similar performance as GCE using GT wireless RT result while outperforming other non-RT based baselines.

VI. CONCLUSION

We propose SANDWICH, an offline, fully differentiable, GPU-trainable wireless RT neural surrogate. By using DT with state supervision and a novel data augmentation technique, we improve model accuracy. Our results show that SANDWICH provides wireless RT prior knowledge similar to a real raytracer in channel modeling. This work paves the way for efficient, reliable wireless RT solutions for JCAS integration.

REFERENCES

- [1] Y. Feng, M. Guenach, et al. “D-Band Channel Modelling by 3D Ray Tracing for Joint Communications and Sensing”. In: *2024 IEEE 4th International Symposium on Joint Communications and Sensing (JC&S)*. IEEE, 2024, pp. 1–6.
- [2] S. Papaioannou, P. Kolios, et al. “Integrated ray-tracing and coverage planning control using reinforcement learning”. In: *2022 IEEE 61st Conference on Decision and Control (CDC)*. IEEE, pp. 7200–7207.
- [3] E. Zhu, H. Sun, et al. “Physics-informed Generalizable Wireless Channel Modeling with Segmentation and Deep Learning: Fundamentals, Methodologies, and Challenges”. In: *arXiv preprint arXiv:2401.01288* (2024).
- [4] J. Hoydis, F. A. Aoudia, et al. “Sionna RT: Differentiable ray tracing for radio propagation modeling”. In: *2023 IEEE Globecom Workshops (GC Wkshps)*. IEEE, pp. 317–321.
- [5] N. Amiot, M. Laaraiedh, et al. “Pylayers: An open source dynamic simulator for indoor propagation and localization”. In: *2013 IEEE ICC*. IEEE, pp. 84–88.
- [6] H. Choi, J. Oh, et al. “WiThRay: A versatile ray-tracing simulator for smart wireless environments”. In: *IEEE Access* 11 (2023), pp. 56822–56845.
- [7] T. Orekondy, P. Kumar, et al. “Winert: Towards neural ray tracing for wireless channel modelling and differentiable simulations”. In: *The Eleventh International Conference on Learning Representations*. 2023.
- [8] W. Tärneberg, A. Fedorov, et al. “Towards Practical Cell-Free 6G Network Deployments: An Open-Source End-to-End Ray Tracing Simulator”. In: *2023 57th Asilomar Conference on Signals, Systems, and Computers*. IEEE, pp. 1000–1005.
- [9] L. Zhang, H. Sun, et al. “Wisegrt: Dataset for site-specific indoor radio propagation modeling with 3d segmentation and differentiable ray-tracing”. In: *2024 International Conference on Computing, Networking and Communications (ICNC)*. IEEE, pp. 744–748.
- [10] T. K. Geok, F. Hossain, et al. “A comprehensive review of efficient ray-tracing techniques for wireless communication”. In: *International Journal on Communications Antenna and Propagation* 8.2 (2018), pp. 123–136.
- [11] J. Hoydis, F. A. Aoudia, et al. “Learning radio environments by differentiable ray tracing”. In: *IEEE Transactions on Machine Learning in Communications and Networking* (2024).
- [12] H. Ling, R.-C. Chou, et al. “Shooting and bouncing rays: calculating the RCS of an arbitrarily shaped cavity”. In: *IEEE Transactions on Antennas and Propagation* 37.2 (1989), pp. 194–205.
- [13] *Advanced electromagnetic ray tracing methods*. www.ee.cit.tum.de/en/hft/forschung/advanced-electromagnetic-ray-tracing-methods/.
- [14] F. A. Aoudia, J. Hoydis, et al. *Instant Radio Maps*. 2024.
- [15] A. Radford. “Improving language understanding by generative pre-training”. In: (2018).
- [16] L. Chen, K. Lu, et al. “Decision transformer: Reinforcement learning via sequence modeling”. In: *NeurIPS* 34 (2021), pp. 15084–15097.
- [17] A. Vaswani. “Attention is all you need”. In: *NeurIPS* (2017).
- [18] X. Zhao, Z. An, et al. “Nerf2: Neural radio-frequency radiance fields”. In: *Proceedings of the 29th Annual International Conference on Mobile Computing and Networking*. 2023, pp. 1–15.
- [19] A. Rogne. *Raytracing in channel model development*. 2022.
- [20] M. K. Samimi and T. S. Rappaport. “3-D millimeter-wave statistical channel model for 5G wireless system design”. In: *IEEE Transactions on Microwave Theory and Techniques* 64.7 (2016), pp. 2207–2225.
- [21] *Remcom - Electromagnetic Simulation Software*. <https://www.remcom.com/>.
- [22] F. Ladhak, E. Durmus, et al. “When do pre-training biases propagate to downstream tasks? a case study in text summarization”. In: *Proceedings of the 17th Conference of the European Chapter of the Association for Computational Linguistics*. 2023, pp. 3206–3219.
- [23] Z. Lai, C. Zhang, et al. “Real-Time Simulation of Wireless Signal Propagation for Dynamic Environment Through GPU-Based Ray Tracing”. In: *Proceedings of the ACM SIGCOMM 2024 Conference: Posters and Demos*, pp. 98–100.
- [24] T. Hehn, M. Peschl, et al. “Differentiable and Learnable Wireless Simulation with Geometric Transformers”. In: *arXiv preprint arXiv:2406.14995* (2024).
- [25] G. Chi, Z. Yang, et al. “RF-Diffusion: Radio Signal Generation via Time-Frequency Diffusion”. In: *Proceedings of the 30th Annual International Conference on Mobile Computing and Networking*. 2024, pp. 77–92.
- [26] J. Knodt, J. Bartusek, et al. “Neural ray-tracing: Learning surfaces and reflectance for relighting and view synthesis”. In: *arXiv preprint arXiv:2104.13562* (2021).
- [27] V. Sitzmann, J. Martel, et al. “Implicit neural representations with periodic activation functions”. In: *NeurIPS* 33 (2020), pp. 7462–7473.
- [28] R. Carr and B. Hulcher. “PATH TRACING: A NON-BIASED SOLUTION TO THE RENDERING EQUATION”. In: *Advanced Graphics Lecture Notes*. 2011.
- [29] A. Keller, T. Viitanen, et al. “Are we done with ray

- tracing?” In: *SIGGRAPH Courses*. 2019, pp. 3–1.
- [30] J. T. Kajiya. “The rendering equation”. In: *Proceedings of the 13th annual conference on Computer graphics and interactive techniques*. 1986, pp. 143–150.
- [31] M. Tancik, P. Srinivasan, et al. “Fourier features let networks learn high frequency functions in low dimensional domains”. In: *NeurIPS* 33 (2020), pp. 7537–7547.
- [32] A. Sobehy, É. Renault, et al. “CSI-MIMO: K-nearest neighbor applied to indoor localization”. In: *2020 ICC (ICC)*. IEEE, pp. 1–6.
- [33] C. Kim, J. Kim, et al. “Dynamics-Augmented Decision Transformer for Offline Dynamics Generalization”. In: *3rd Offline RL Workshop: Offline RL as a “Launchpad”*.
- [34] Y. Ma, H. Jianye, et al. “Rethinking decision transformer via hierarchical reinforcement learning”. In: *ICML*. 2023.
- [35] K. Paster, S. McIlraith, et al. “You can’t count on luck: Why decision transformers and rvs fail in stochastic environments”. In: *NeurIPS* 35 (2022), pp. 38966–38979.
- [36] X. Wang, K. Guan, et al. “Graph Neural Network enabled Propagation Graph Method for Channel Modeling”. In: *IEEE Transactions on Vehicular Technology* (2024).
- [37] W. Wu, X.-M. Fu, et al. “Data-driven Interior Plan Generation for Residential Buildings”. In: *ACM Transactions on Graphics (SIGGRAPH Asia)* 38.6 (2019).